

Feasibility of a down-scaled HEMP-Thruster

IEPC-2011-138

*Presented at the 32nd International Electric Propulsion Conference,
Wiesbaden, Germany
September 11–15, 2011*

Andreas Keller*

*University of Giessen, I. Physikalisches Institut, 35392 Giessen, Germany
Astrium GmbH - Satellites, 88039 Friedrichshafen, Germany*

Peter Köhler, Waldemar Gärtner, Benjamin Lotz and Davar Feili

University of Giessen, I. Physikalisches Institut, 35392 Giessen, Germany

Philipp Dold, Marcel Berger

Astrium GmbH - Satellites, 88039 Friedrichshafen, Germany

Claus Braxmaier

HTWG Konstanz, Institute for Optical Systems, 78462 Konstanz, Germany

and

Dennis Weise, Ulrich Johann

Astrium GmbH - Satellites, 88039 Friedrichshafen, Germany

New satellite missions require increasing precision attitude and orbit control combined with long life time. The HEMP (High Efficiency Multistage Plasma) thruster technology has promising properties in the mN thrust range with respect to system simplicity and erosion. We investigate experimentally the ability of down-scaling the HEMP thruster concept into the μ N thrust range. This means building up and testing of thruster hardware as well as verification of simple models. Numerical simulation and optimisation of thruster operation is complementary aspect of the work. We present the relevant design considerations and the test setup. First results of an experimental comparison of two different configurations are presented which differs with respect to ferromagnetism of the housing and shielding of the magnetic field of permanent magnets.

Nomenclature

HEMPT = High Efficiency Multistage Plasma Thruster
HET = Hall Effect Thruster
RPA = Retarding Potential Analyser
LISA = Laser Interferometer Space Antenna

*Andreas.Keller@exp1.physik.uni-giessen.de

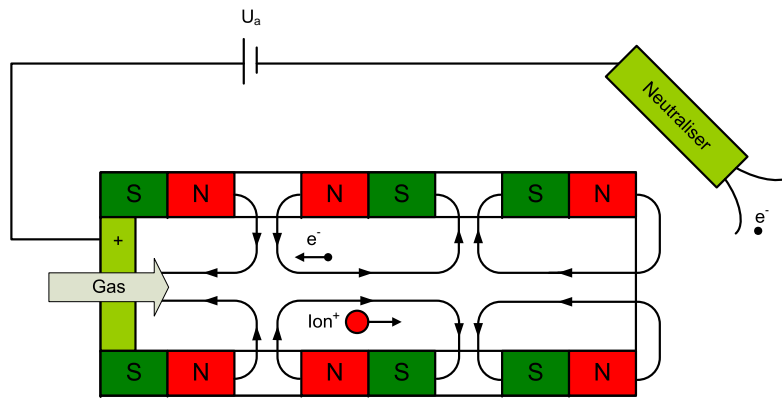


Figure 1. HEMPT principle, U_a denotes the anode voltage

I. Introduction

For the planned LISA mission the need for high precision attitude and orbit control creates the demand of new thruster technologies with thrust in the μN -region and low noise, in combination with a long life time. A possible candidate is the HEMP thruster, which is a promising concept with respect to system simplicity and life time.

This work studies the application of the HEMP thruster technology for the LISA and similar missions in experiment. For this purpose a number of thruster prototypes were built, tested and characterised.

II. Design of thrusters

The HEMP thruster is based on the principle of electron bombardment ionisation and ion acceleration in the same electric field, generated by the anode (see Fig. 1). The ring shaped periodically poled permanent magnets create several cusp areas with radial magnetic field, where the electrons oscillate on Larmor radii to increase the interaction length and to reduce wall erosion. For the detailed concept it is referred to Ref. 1 and Ref. 2.

The thrusters consists of a cylindrical discharge chamber of alumina and three SmCo magnets which have a high temperature capability in combination with a high magnetic field and space qualification. In order to achieve a low thrust with a high specific impulse it is required to decrease the mass flow which results in a lower gas pressure in the discharge chamber. A lower pressure results in a lower ionisation efficiency which can lead to a breakdown of plasma generation. The reduction of chamber diameter counteracts the decrease of pressure with lower mass flow.

The latest thruster model have been realised with the same geometry in three different housing materials: Dielectric (a MACOR ceramics, see a photograph of complete thruster in Fig. 2), electrically conducting but paramagnetic (aluminum) and electrically conducting and ferromagnetic (steel 1.0711).

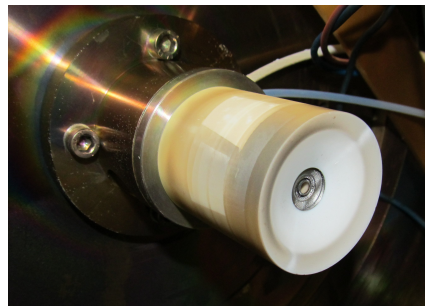


Figure 2. μHEMP thruster with ceramics housing

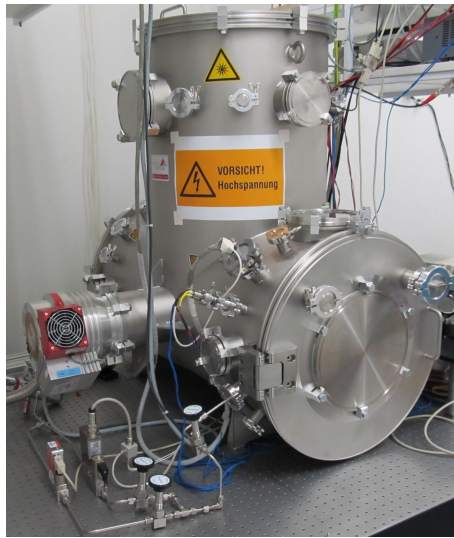


Figure 3. Test facility at Astrium GmbH

A ferromagnetic housing can influence the plume as published for hall effect thrusters in Ref. 3. It shields the magnetic field outside the thruster and hinders the electrons from oscillating on Larmor radii in front of the exit plane. These could create a ring shaped electric charge which acts attracting to the ions resulting in a larger angle of beam as a possible explanation.

The other parts of the thruster are identical, for neutraliser and electron source an incandescent lamp is used which is placed outside the thruster a few centimeters away.

III. Operation

The operational parameter space has been initially characterised at the test facility at Astrium GmbH (see Fig. 3). It consists of a T-shaped vacuum chamber with a length of 1 m, a diameter of 50 cm and a volume of 300l, placed on a damped optical table . A turbo-molecular pump is mounted with a throughput of 700l/s.

Fig. 4 shows the observed operation parameter space of power (anode voltage times anode current

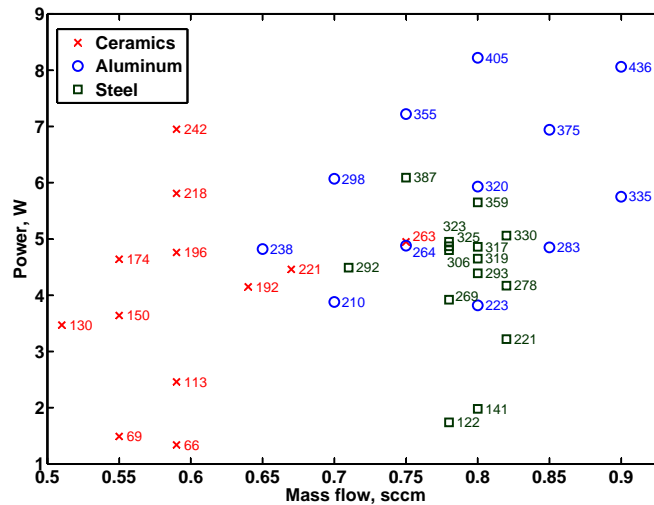


Figure 4. Operation parameter space for the three different thruster types. The numbers on the right side of data points denotes the calculated thrust in μN .

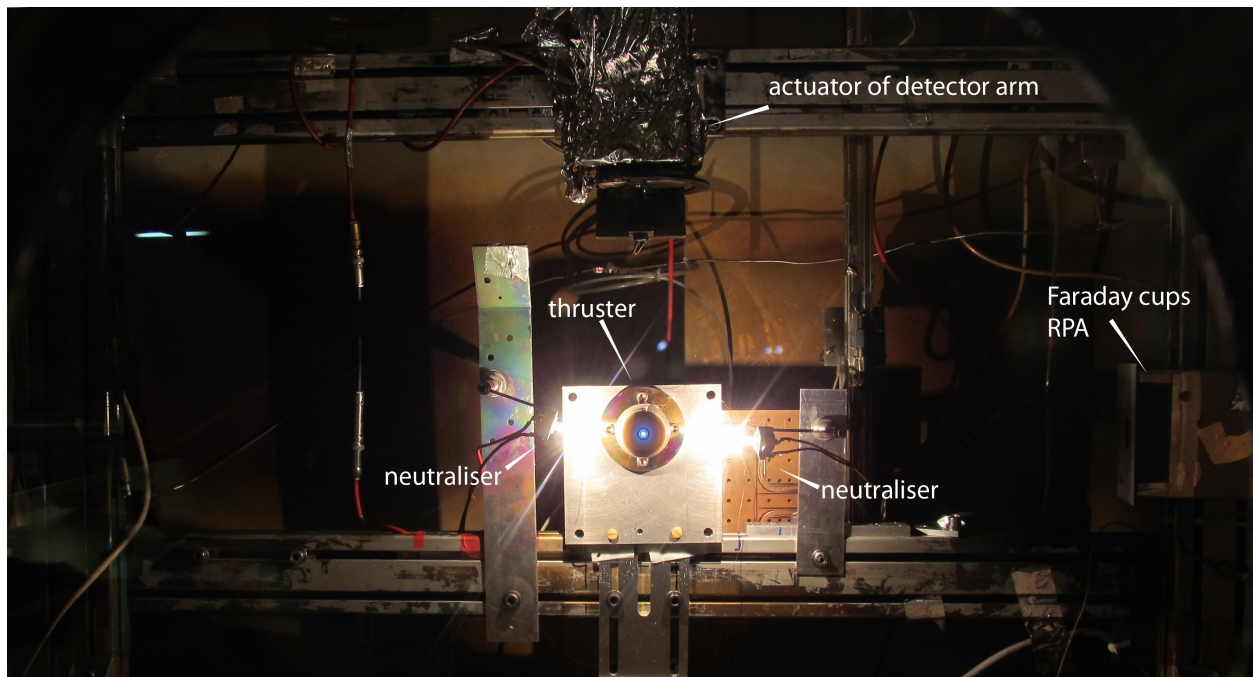


Figure 5. Thruster (center) with two neutraliser incandescent lamps (left and right) and Faraday Cup / RPA detector (rightmost). The actuator of detector arm and rotation axis is shown in the top center position.

measured by power supply) and mass flow (measured by Bronkhorst F-200CV) of the three different thruster types. Each data point denotes a measurement of minimum two hours of constant operation, the calculated thrust is written in μN on the right side of the point. These points represent the lower limit of operation with respect to power and mass flow.

The ceramics thruster demonstrates the lowest thrust with $70 \mu\text{N}$ in combination with low power consumption and mass flow. The corresponding specific impulse is 125 s , while for higher thrust values ($150 - 430 \mu\text{N}$) points are between $300 - 580 \text{ s}$. These values were calculated with the divergence efficiencies measured in the next section. The minimal power, minimal mass flow and minimal thrust is higher for the aluminum thruster. The steel thruster is in between with respect to minimum thrust, although the minimum mass flow is slightly higher.

IV. Characterisation

Plume properties were characterised with Faraday cups and a Retarding Potential Analyser in the BigMac test facility at university of giessen. It is a cylindrical vacuum chamber with a diameter of 1.6 m and a length of about 1 m . The pumping system has a maximum throughput of 25000 l/s and consists of turbo molecular and cryopumps.

A mechanical arm with an arm length of 40 cm is installed, which can be rotated by 180° around the thruster. In this plane there is an array of eight encapsulated Faraday cups and a Retarding Potential Analyser (RPA) mounted. The Faraday cups are distributed on a line perpendicular to the plane with a separation of 1 cm each. The open surface of the cups is a circle with a diameter of 3.2 mm .

The RPA consists of an ion detector with three upstream grids which repel and suppress the neutraliser electrons, the slow ions and secondary electrons generated in the detector, respectively. By successive increasing of the retarding voltage more and more ions are repelled from detector at the second grid, so that the derivative of ion current is a measure of distribution of ions which passed a given acceleration voltage.

An image of operating thruster in BigMac test facility is shown in Fig. 5. The thruster in the center is surrounded by two neutraliser and on the right edge the Faraday Cups / RPA detector is visible.

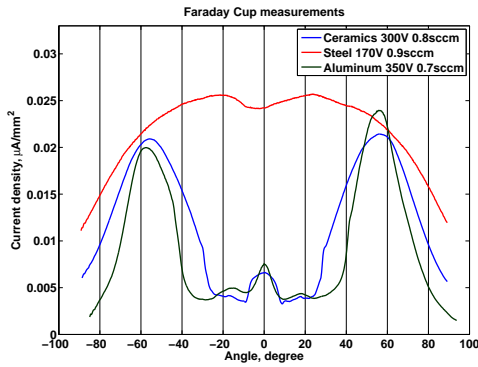


Figure 6. Faraday cup measurements for three different thruster types (ceramics, ferromagnetic steel and aluminum housing) at different operation points.

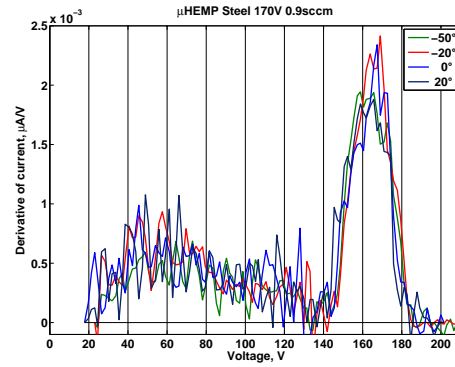


Figure 7. RPA measurement of steel thruster at four different angles.

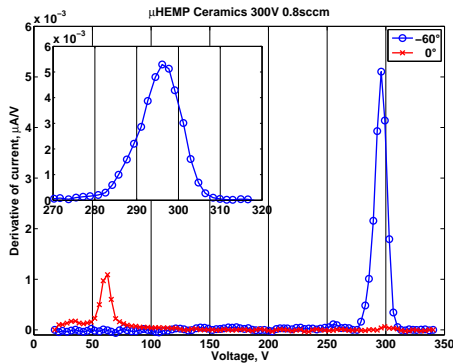


Figure 8. RPA measurement of ceramics thruster at two different angles. In the inset a detail measurement with higher sample rate is shown.

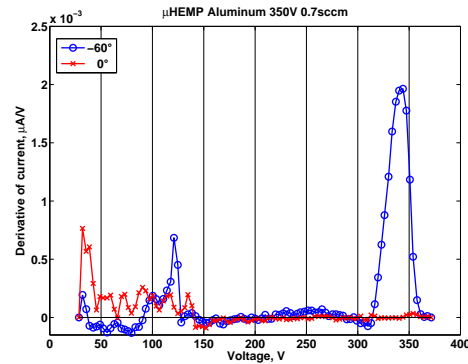


Figure 9. RPA measurement of aluminum thruster at two different angles.

1. Faraday cup measurements

The results of Faraday array measurements are given in Fig. 6. The current density measured with one cup is plotted against angular position for the three different thruster types. The ceramics and the aluminum thruster shows side lobes with a maximum of ion emission near 60° . Due to a higher environmental pressure and a slight asymmetry of neutraliser position the asymmetry of the aluminum measurement can be explained. The post processing shifts the balance point of the whole measurement to the center except for aluminum measurement at which the small center peak was moved to 0° .

In consistency with the work³ on HETs, the ion distribution of the ferromagnetic steel thruster shows one peak at the center, although much broader. This single peak behaviour is due to the ferromagnetic structure of the housing since the electrically conducting but paramagnetic aluminum housing shows a similar distribution to the ceramics thruster.

In Table 1 the derived data of total ion current, divergence efficiency η_{div} and angle of aperture ν_{90} (divergence angle of 90% of ions), thrust (with the assumption of 10% doubly ionised ions) and specific impulse are given. The broad main peak of steel thruster does increase divergence efficiency only marginally (about 4%) in comparison with aluminum thruster which can be explained by the ion emission at high angles having a high solid angle. The high angle of aperture ν_{90} of 79.4° is a measure for this behaviour.

2. Retarding Potential Analyser

The results of RPA measurements for different angles with non-zero ion intensity are given in Fig 7 - 9. The derivative of ion current is plotted against retarding voltage. In Fig 8 the results of the ceramics thruster

Thruster	Anode Voltage (V)	Mass flow (sccm)	Ion current (mA)	Divergence efficiency η_{div}	Angle of aperture ν_{90} ($^{\circ}$)	Thrust (μN)	I_{sp} (s)
Ceramics	300	0.8	13.7	0.518	78.0	200	280
Steel	170	0.9	23.6	0.573	79.4	280	350
Aluminum	350	0.7	10.4	0.537	74.5	170	270

Table 1. Thruster data of measurements presented

with an anode voltage of 300 V is shown for 60° and 0° (directly in thruster direction). While the main part of ions at 60° passed the full potential difference of 300 V, the ions at 0° passed a much lower voltage of 60 V, which can be explained that at 60° all ions are created in the upstream cusp (near the anode) and at 0° in the downstream cusp (near the exit). The three magnets generate two cusp areas while the main potential drop occurs in the anode cusp (see Ref. 1, Fig. 6.16).

The results for different angles of the ferromagnetic steel thruster are shown in Fig. 7 with an anode voltage of 170 V. It is evident that the ion acceleration voltage distribution is independent of angle, the main part of ions have passed 170 V and a minor part passed about 60 V. The low voltage ions can possibly be due to a higher chamber pressure in comparison to the ceramics measurement (momentum and charge exchange collisions of fast ions with thermal neutral gas) since the peak is very broad.

The results of the aluminum thruster (see Fig. 9) shows similar results in comparison to the ceramics case. The broad peak of low voltage ions at 0° can be explained by the higher chamber pressure while the peak at 60° and 120 V can be due to ionisation in the downstream cusp.

The high acceleration voltages points to a high acceleration efficiency for all three thruster types so that the non-uniformity of ion acceleration voltages can be neglected on thrust and specific impulse calculations.

V. Conclusion

In this publication measurements of three μHEMP thruster prototypes for down-scaling are presented. All three thruster types function properly. A positive effect of single peak ion distribution of the steel thruster for the divergence efficiency is observed. Further optimisations and increase of divergence efficiency are envisaged. The single peak ion distribution is an effect of ferromagnetic structure of housing material and not the electrically conducting feature of the metal. The acceleration is very efficient since nearly all ions passed the complete potential difference.

A stable operation was possible down to 70 μN so that it appears realistic to reach with further geometric changes of chamber diameter and magnets the low two-digit μNewton thrust range with reasonable specific impulse. Both concepts, the ferromagnetic and dielectric housing, are continued and tested with respect to scalability and divergence efficiency.

Further efforts for thrust reduction and efficiency optimisation are to be performed to show the potential of this thruster principle as a candidate for LISA and similar missions.

References

- ¹H. Bassner, R. Killinger, J. Mitterauer, F. Rüdener, N. Koch, and G. Kornfeld. *Vacuum Electronics*. Springer Berlin Heidelberg, 2008.
- ²G. Kornfeld, N. Koch, and H.P. Harmann. Physics and evolution of hemp-thrusters. 30th International Electric Propulsion Conference, 2007. IEPC-2007-108.
- ³Y. Raitses, J.C. Gayoso, E. Merino, and N.J. Fisch. Effect of the Magnetic Field on the Plasma Plume of the Cylindrical Hall Thruster with Permanent Magnets. 2010.